Kicked rotor and Anderson localization

Boulder School on Condensed Matter Physics, 2013

Dominique Delande
Laboratoire Kastler-Brossel, Université Pierre et Marie Curie, Ecole Normale Supérieure, CNRS; 4 Place Jussieu, F-75005 Paris, France

CONTENTS

INTRODUCTION: ANDERSON LOCALIZATION

The physics of Anderson localization is highly dependent on the dimension of the system. While the 1d situation is fairly well understood—localization is the generic behavior, the localization length is comparable to the mean free path, and the fluctuation properties in the localized regime are essentially well understood—the physics of higher dimensions is much richer still. Dimension 3 is especially interesting, as one expects a so-called mobility edge, separating in the continuum case localized states at low energy/strong disorder from extended states at high energy/weak disorder.

It is however rather difficult to find a clean experimental system to observe this metal-insulator Anderson transition unambiguously. Cold atomic matter waves are very attractive because they can be directly observed, and because most experimental imperfections as well as atom-atom interactions can be precisely controlled, if not reduced to a minimum.

To start with a specific, state-of-the-experimental-art example, imagine a one-dimensional non relativistic particle evolving in a potential $V(z)$ as depicted in Fig. 1. The evolution of the wavefunction $\psi(z,t)$ is given by Schrödinger's equation:

$$i\hbar\partial_t\psi(z,t) = H\psi(z,t) \tag{1}$$

with the single-particle Hamiltonian

$$H = \frac{p^2}{2m} + V(z). \tag{2}$$

Let us assume that the particle is initially prepared in a Gaussian wave-packet. In the absence of any potential, the Gaussian wave-packet will show ballistic motion, where the center of mass moves at constant velocity while the width

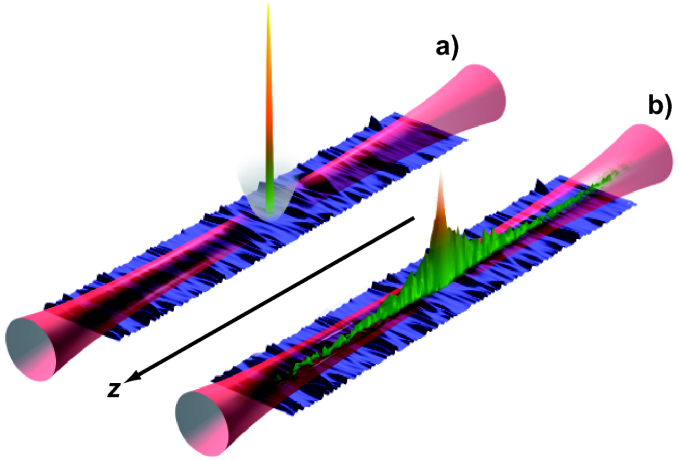

FIG. 1. Direct experimental observation of one-dimensional Anderson localization of an atomic matter wave in a disorder potential. The disorder potential (represented in blue in the lower part of the figure) is created by a speckle pattern. (a) An initially localized wave packet (prepared in a harmonic trap at the center) evolves freely, diffuses and eventually freezes at long times in a characteristic exponential shape (b). The pink tube represents the transverse-confinement laser beam that ensures an effectively one-dimensional dynamics. Reprinted from [1] (courtesy of Ph. Bouyer).

increases linearly with time at long times. In the presence of a certain realization $V(z)$ of the disorder, the wave function will take a certain form $\psi(z,t)$. For different realizations, different wave functions will be obtained. But we are not interested in the fine details of each wave function. Rather, we wish to understand the generic, if not universal, properties of the final stationary density distribution $|\psi(z)|^2$ obtained at long times.

Let us forget for a moment interference effects and try to guess what happens to a classical particle. If its kinetic energy is much larger than the typical strength of the disorder V_0, the particle will fly above the potential landscape, and the motion is likely to be ballistic on the average. If on the other hand V_0 is larger than the kinetic energy, the particle will be trapped inside a potential well and transport over long distance is suppressed, i.e. localization takes place.

Quantum mechanics modifies this simple picture fundamentally: waves can both tunnel through potential hills higher than the kinetic energy and be reflected even by small potential fluctuations. So the initial wavepacket will split on each potential fluctuation into a transmitted part and a reflected part, no matter how large the kinetic energy with respect to the potential strength may in detail be. After many scattering instances, this looks like a random walk and one naïvely expects that, on average, the motion at long times will be diffusive, with a diffusion constant depending on some microscopic properties of particle and potential.

This simple model system has been recently realized experimentally [1] using a quasi-one-dimensional atomic matter wave, interacting with an effective optical potential created by a speckle pattern, see Fig. 1. The experimental result is the following: at short times, the wavepacket spreads as expected, but at long times, its average dynamics freeze, and the wavepacket takes a characteristic exponential shape:

$$|\psi(z)|^2 \propto \exp\left(-\frac{|z|}{\xi_{\rm loc}}\right) \tag{3}$$

where $\xi_{\rm loc}$ is called the localization length [18]. Moreover, if a different realization of the disorder is used (i.e. a microscopically different, but statistically equivalent speckle pattern), an almost identical shape is obtained, meaning that the phenomenon is robust versus a change of the microscopic details.

This surprising phenomenon is known as Anderson localization, sometimes also called strong localization. Although it was predicted on theoretical grounds in the late 50's—most famously by P.W. Anderson himself [2]—it has only been observed directly rather recently. Cold atoms, where an *in situ* direct observation of the wavefunction is possible, are from that point of view highly valuable.

While Anderson localization is the generic scenario in 1d — and also in 2d for time-reversal invariant systems – the physics is richer in 3d and higher dimensions. There is a so-called mobility edge, that is an energy below which all states are localized and above which all states are delocalized and where the temporal dynamics at long time is diffusive.

The scaling theory of localization [3](a one-parameter scaling law) correctly predicts the existence of a metal/insulator (or diffusive/localized) transition in 3d. A scaling theory can hope to capture those features that are important

on macroscopic scales, but will be insensitive to microscopic details. This means that its predictions are only semi-quantitative, in the sense that it cannot furnish the precise location of a critical point in parameter space nor provide any system-specific data. In return, if one feeds it with the microscopic data (such as the transport mean-free path), it can give general, and surprisingly accurate, predictions of universal character. The position of the critical point is given by the so-called Ioffe-Regel which relates the wavevector k of the particles and the mean-free path l in the presence of the disorder:

$$kl \approx 1 \tag{4}$$

The precise value of the critical kl depends on microscopic details and is therefore non universal.

The behavior of the β-function around the critical point yields precious information about the large-scale physics, and permits especially to calculate *critical exponents* that are the hallmark of universality. In their 1979 paper, Abrahams et al.[3] showed that the localization length diverges close to the transition for $W > W_c$ as

$$\xi_{\rm loc} \sim (W - W_c)^{-\nu}, \tag{5}$$

where W is a control parameter (for example the energy) and W_c its value at the critical point (that is the mobility edge if W is the energy).

The critical exponent $\nu = 1/s$ is determined by the slope of the β-function at the transition, $s = [{\rm d}\beta/{\rm d}\ln g]_{g_c}$. This critical exponent is *universal* that is independent of the microscopic details and depends only on the dimension and the symmetry properties of the system.

While Anderson localization in 1d does not require a strong disorder (the mean-free path is 100 times the atomic de Broglie wavelength in the experiment discussed above), the situation is completely different in 3d, as one needs both small k (low energy, large de Broglie wavelength) and short mean free path l. Indeed, the latter cannot be shorter than the correlation length of the disordered potential, i.e. of the order of 1 μm for optical speckle. Although two experimental observations of Anderson localization with 3d atomic matter waves have been reported [4, 5], none of these observations is really convincing. Because of strong disorder, the state of the system is not well controlled: states below and above the mobility edge are simultaneously populated, the position of the mobility edge itself is not precisely known, making the characterization of the Anderson transition and the measurement of the critical exponent a very difficult task, not yet achieved.

This limitation on the mean free path can be overcome using a different approach, where disorder is not provided by an external potential in configuration space, but by classically chaotic dynamics in momentum space. The disorder is there provided by the free temporal dynamics of the system and can be easily modified. This idea has been realized experimentally with the atomic kicked rotor, and Anderson localization in 1d has been observed as early as 1994 [6], 14 years prior to the widely noticed Anderson localization in configuration space [1]! A key advantage of the kicked rotor is that is does not require ultra-cold atoms from a Bose-Einstein condensate: a standard magneto-optical trap suffices to prepare the initial state.

In these lectures, I will discuss in details the properties of the kicked rotor. In particular, conveniently tailoring the temporal excitation of the kicked rotor has permitted the clean observation of the metal-insulator Anderson transition in 3d, the first experimental measurement of the critical exponent with non-interacting matter waves [7], the experimental demonstration of its universality [8], as well as a detailed study of the critical regime [9].

In Lecture I, I introduce the periodically kicked rotor, which displays a phenomenon known as dynamical localization, and show that it is nothing but 1d Anderson localization in momentum space.

Experiments on the periodically kicked rotor are discussed in Lecture II, with emphasis on all experimental imperfections which could spoil Anderson localization and how to overcome them, a key point towards the observation of the Anderson transition in 3d.

In Lecture III, I discuss the quasi-periodically kicked rotor, which displays an equivalent of the 3d metal/insulator Anderson transition, but in a 1d momentum space. I describe how to analyze experimental results in order to show that it is a true quantum phase transition and not a cross-over, how to measure the critical exponent, how to test its universality and how to characterize the critical regime.

Note: with the lecture notes, I provide a set of computer scripts written in the Python language, available at http://boulderschool.yale.edu/news/delandes-python-code-download. They can be used to perform numerical experiments on the kicked rotor (both the classical and the quantum kicked rotors). The reader is encouraged to play with them, modify them to produce new results. The goal is to get some insight in the fundamental physical processes at work. Seeing is believing! Of course, it cannot provide us with *explanations* (from this point of view, numerical experiments are like real experiments), it can just be used as a testing ground for new ideas.

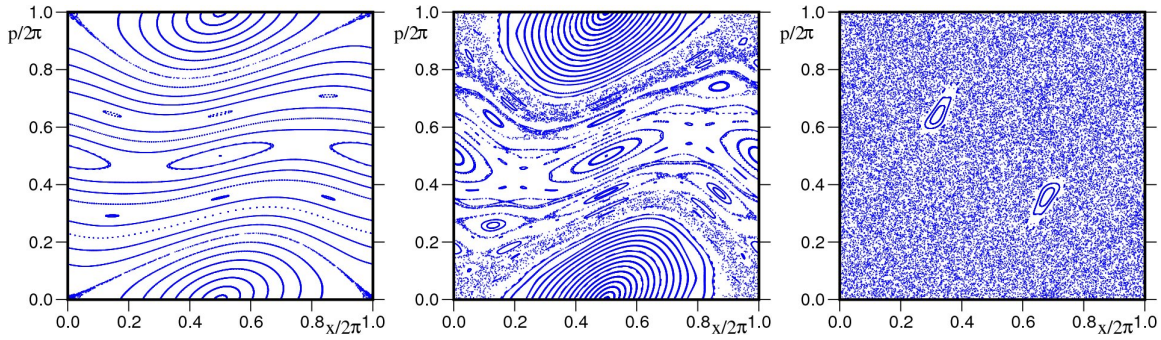

FIG. 2. Poincaré surfaces of section for the standard for $K = 0.5,\ 0.97$ and 5 (from left to right), showing the progressive onset of chaos (from Scholarpedia).

The scripts can be ran on any computer where Python is installed. It requires the standard scientific packages numpy and scipy. These are usually installed on Linux computers, or installation is more or less straightforward (depending on the Linux distribution used). Python can be installed on practically any computer, see http://www.python.org/download/. For M$-Windoze users, Enthought Canopy (https://www.enthought.com/products/canopy/) has a free version including numpy and scipy.

The scripts just produce numerical data, but no way of visualizing them. Please use your favorite plotting software.

The time needed to run these scripts has been kept to a minimum, of the order of 10 seconds on a ordinary laptop. Of course, it may take longer if you modify the parameters...

I. LECTURE I: THE PERIODICALLY KICKED ROTOR

A. The model

We consider a one-dimensional rotor whose position can be described by the angle x (defined modulo 2π) and the associated momentum p, and kick it periodically with a position-dependent amplitude. In properly scaled units, the Hamiltonian function can be written as

$$H = \frac{p^2}{2} + k\cos x \sum_{n=-\infty}^{+\infty} \delta(t - nT) \tag{6}$$

where T and k are period and strength of the kicks, respectively.

B. Classical dynamics

Because of the time-dependence, energy is not conserved, but thanks to the time-periodicity, we can analyze the motion stroboscopically and build a Poincaré map picturing the evolution once every period. This map relates the phase space coordinates just before kick $n+1$ to the coordinates just before kick n:

$$\begin{cases} I_{n+1} = I_n + K\sin x_n \\ x_{n+1} = x_n + I_{n+1} \end{cases} \tag{7}$$

where $K = kT$ and $I_n = Tp_n$. This is nothing but the celebrated standard map (also known as the Chirikov map) that has been widely studied [10, 11]: it is almost fully chaotic and ergodic around $K = 8$ and above, see fig. 2.

Note: The scripts `standard_map_single_trajectory.py` and `standard_map_several_trajectories.py` compute the iterates of a single and several initial points, respectively. The first script shows whether an initial condition is regular (all iterates lie on a line) or chaotic (it fills densely part of the plane). The second script generates a Poincaré surface of section.

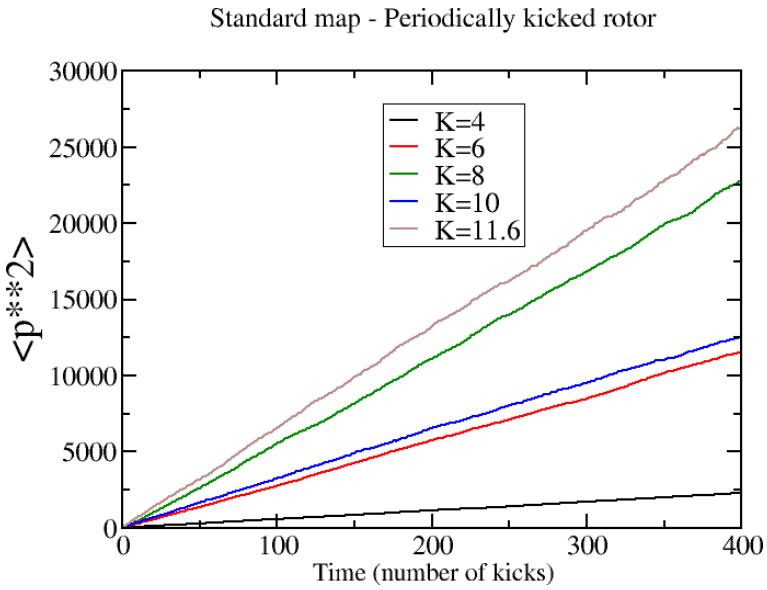

FIG. 3. Evolution of $\langle p^2 \rangle$ as a function of time, showing a diffusive behaviour, for sufficiently large values of K. $\langle p^2 \rangle$ is averaged over a family of initial conditions.

C. Chaotic diffusion

At each kick, the momentum changes by a quantity $k \sin x_n$ which can be either positive or negative. When the stochasticity parameter K is very large, each kick is so strong that the positions of the consecutive kicks can be taken statistically uncorrelated. The momentum p then receives kicks with a pseudo-random amplitude, resulting in a random walk in momentum space. Not surprisingly, this induces a global diffusive-like behaviour, see fig. 3, although the motion is perfectly deterministic. By averaging and assuming consecutive kicks to be uncorrelated, we obtain:

$$\langle p_{n+1}^2 \rangle \simeq \langle p_n^2 \rangle + k^2 \langle \sin^2 x_n \rangle \simeq \langle p_n^2 \rangle + \frac{k^2}{2} \tag{8}$$

It follows that the motion in momentum space is indeed diffusive, $\langle p^2 \rangle = 2Dt$ increases linearly with time. The diffusion constant depends on k and is approximately given by:

$$D = \frac{k^2}{4T}. \tag{9}$$

The numerical results are in good overall agreement with this prediction, see fig. 4. There are however oscillations due to residual correlations between consecutive kicks. They can be computed leading to the improved expression:

$$D = \frac{k^2}{4T}(1 - 2J_2(K) + 2J_2^2(K)) \tag{10}$$

with J_2 the ordinary Bessel function. This expression is in excellent agreement with the numerical results, see fig. 4. Note however the extra sharp peaks immediately above integer multiples of 2π. These are due to the so-called "accelerator modes". For $K = 2\pi$, it is easy to check that there is a trajectory such that $x_n = \pi/2 + n(n+1)\pi$, $p_n = 2n\pi$ where the momentum increases ballistically. For K slightly larger than $2m\pi$, there are trajectories trapped in an accelerating island. Although they occupy only a small fraction of phase space, they give diverging contributions to the diffusion constant. This can be considered as a pathology of the model without any serious consequence.

Note that the kicked rotor is a perfectly deterministic system, without any randomness. It is the chaotic nature of the classical motion, and thus its extreme sensitivity to perturbations, which renders the deterministic classical motion diffusive *on average*.

Note: the script `standard_map_final_momentum_distribution.py` generates the distribution of final momentum starting from a ensemble of trajectories initially located near $p = 0$. `standard_map_p2_vs_time.py` shows the linear increase of $\langle p^2 \rangle$ with time. `standard_map_diffusion_constant_versus_K.py` computes the diffusion constant (with error bars) as a function of K. Warning: this script is the only one requiring a rather long execution time (around 15 minutes).

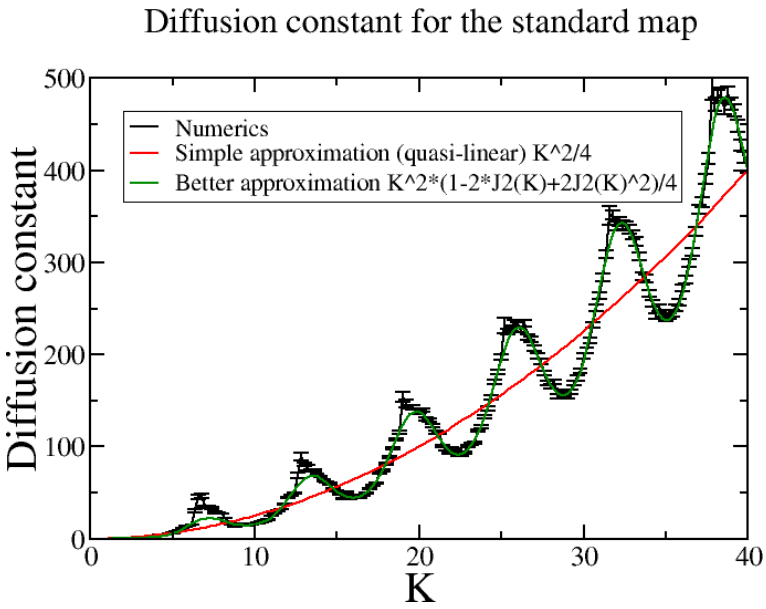

FIG. 4. Diffusion constant for the kicked rotor (standard map) as function of the stochasticity parameter K. It is growing like $K^2/4$ with oscillations. Note the peaks near integer multiple of 2π related to the so-called "accelerator" modes.

D. Quantum dynamics

The quantum Hamiltonian is obtained from the classical one, eq. (6), through the canonical replacement of p by $-i\hbar\partial_x$.

The evolution operator over one period is the product of the free evolution operator and the instantaneous kick operator:

$$U = U(T,0) = \exp\left(-\frac{i}{\hbar}\frac{p^2 T}{2}\right)\exp\left(-\frac{i}{\hbar}\,k\cos x\right) \tag{11}$$

The long-time dynamics is generated by successive iterations of U. Thus, one can use the eigenstates of U as a basis set. U being unitary, its eigenvalues are complex numbers with unit modulus:

$$U|\phi_j\rangle = \exp\left(-\frac{iE_j T}{\hbar}\right)\,|\phi_j\rangle \tag{12}$$

with $0 < E_j \leq 2\pi\hbar/T$ are defined modulo $2\pi\hbar/T$. They are not exactly the energy levels of the system—the $|\phi_j\rangle$ are not stationary states of the time evolution, but are only periodic—and are called quasi-energy levels, the $|\phi_j\rangle$ being the Floquet eigenstates. This Floquet description is the time-analog of the Bloch theorem, that applies to spatially periodic potentials. The Floquet theorem implies that any solution of the time-dependent Schroedinger equation can be written as a linear combination of $\exp(-iE_j t/\hbar)\;|\phi_j(t)\rangle$.

Because of the spatial periodicity, the natural basis states are the eigenstates $|m\rangle$ of the p operator labelled with the integer quantum number m:

$$\langle\theta|m\rangle = \frac{\exp(im\theta)}{\sqrt{2\pi}} \tag{13}$$

They are eigenstates of p^2 with the eigenvalue $m^2\hbar^2$.

The Floquet eigenstates can be obtained by numerical diagonalization of U, whose matrix elements in the momentum eigenbasis, are quite simple:

$$\langle m'|U|m\rangle = (-i)^{m-m'}\;J_{m-m'}(K/\hbar)\exp\left(-i\frac{m'^2\hbar}{2}\right) \tag{14}$$

Figure 5 shows typical eigenstates of U obtained numerically. The remarkable properties is that they are all localized in momentum space, with an average exponential decay (with large fluctuations) away from the center of localization. It should also be noted that the localization length does not depend on the position of the center of localization.

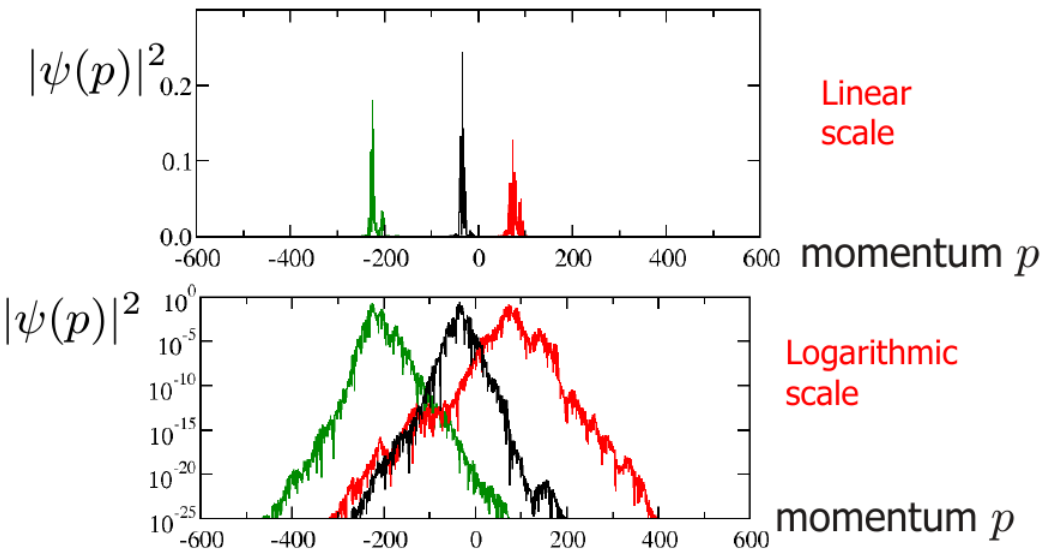

FIG. 5. Three typical Floquet eigenstates displaying exponential localization in momentum space.

Note: the script `kr_Floquet_eigenstates.py` diagonalizes the (truncated) evolution operator in momentum basis, producing the spectrum (mainly on the unit circle) and the localized Floquet eigenstates.

E. Dynamical Localization

The quantum dynamics of the kicked rotor can be quite simply studied numerically by repeated application of the one-period evolution operator U to the initial state, alternating free propagation phases with instantaneous scattering events in momentum space induced by the kicks. The free evolution between kicks, $\exp\left(-ip^2T/2\hbar\right)$, is diagonal in momentum representation, such that each momentum eigenstate, characterized by its momentum $m\hbar$ with integer m, picks up a different phase shift. The kick operator $\exp\left(-ik\cos\theta/\hbar\right)$, in contrast, is diagonal in position representation and couples different momenta.

For sufficiently large $K = kT$, the classical dynamics is diffusive in momentum space, but it should come as no surprise to the reader familiar with 1d Anderson localization, that the quantum dynamics may be localized at long times, see figure 6. It is characterized by the saturation of $\langle p^2\rangle$ at long time — in strong contrast with the classical unlimited growth — and by the exponential shape of the density in momentum space, see figure 7, very much like the usual Anderson localization in configuration space. This localization was baptized "dynamical localization" when it was observed in numerical simulations [12]. Only later, people realized that it is nothing but the Anderson scenario of 1d localization, as explained below.

Note: The script `kr_periodic.py` computes the temporal evolution over many kicks, starting from either a single state or averaging over several states. It outputs both $\langle p^2(t)\rangle$ and the probability density in momentum space $\langle|\psi(p)|^2\rangle$ at the final time.

F. Link with Anderson localizations

So far, we have only made plausible that dynamical localization with the quantum kicked rotor is similar to Anderson localization in a spatially disordered medium. We now demonstrate the connection between the two phenomena, following [13]. Consider the evolution operator, eq. (11), and the associated eigenstate $|\phi\rangle$ with quasi-energy E. The part of the evolution operator associated with the kick can be written as:

$$\exp\left(-\frac{i}{\hbar}\,k\cos x\right) = \frac{1+iW(x)}{1-iW(x)} \tag{15}$$

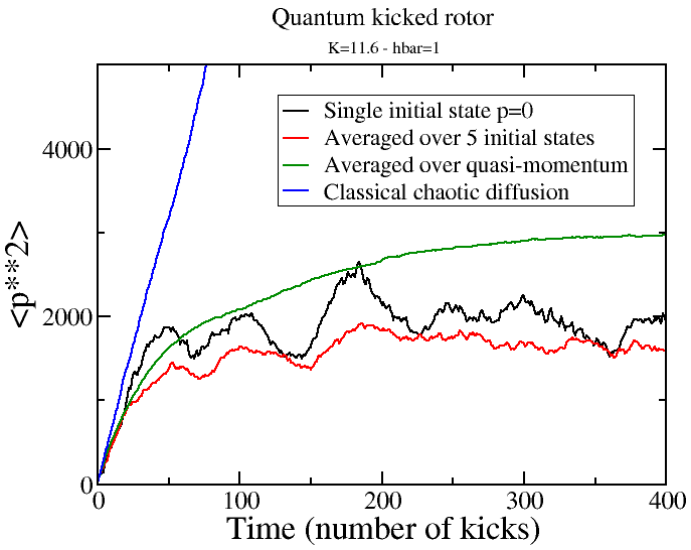

FIG. 6. The expectation value $\langle p^2(t)\rangle$ for the quantum periodically kicked rotor, displaying a diffusive behavior at short time (following the classical dynamics) and saturation at long time. For a single "realization" (a given initial state), there are large fluctuations at long time, which are smoothed out when averaging over possible initial states. Parameters are $K = 11.6, \hbar = 1.0$

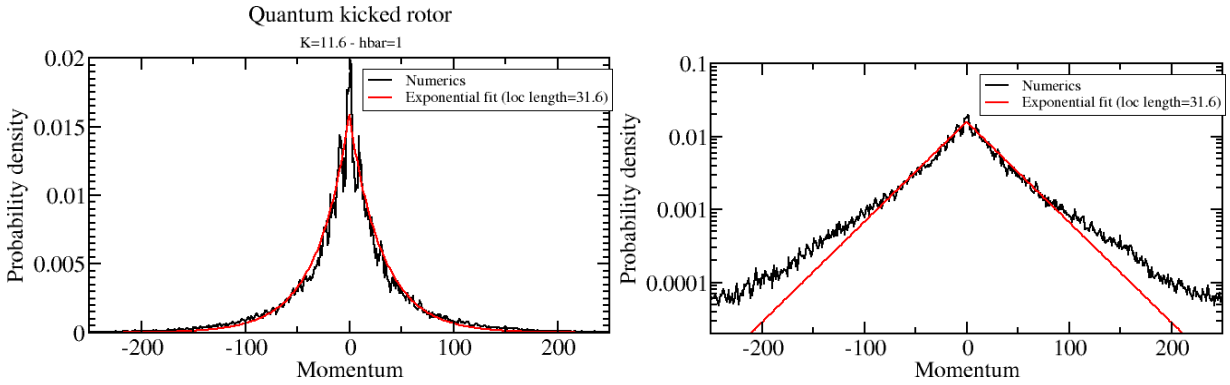

FIG. 7. The average probability density in momentum space $|\psi(p)|^2$ for the quantum kicked rotor after it reaches dynamical localization (after 400 kicks). It displays an average exponential localization with large fluctuations. Parameters are $K = 11.6, \hbar = 1.0$

where $W(x)$ is a periodic Hermitean operator which can be Fourier-expanded:

$$W(x) = \sum_{r=-\infty}^{\infty} W_r \ \exp(irx). \tag{16}$$

Similarly, the kinetic part can be written as:

$$\exp\left[-\frac{i}{\hbar}\left(\frac{p^2}{2} - E\right)\ T\right] = \frac{1+iV}{1-iV} \tag{17}$$

The operator V is diagonal is the eigenbasis of p, labeled by the integer m (see above). If one performs the following expansion in this basis set,

$$\frac{1}{1-iW(x)}|\phi\rangle = \sum_m \chi_m \ |m\rangle, \tag{18}$$

it is straightforward to show that the eigenvalue-equation (12) can be rewritten as

$$\epsilon_m \chi_m + \sum_{r\neq 0} W_r \chi_{m-r} = -W_0 \chi_m \tag{19}$$

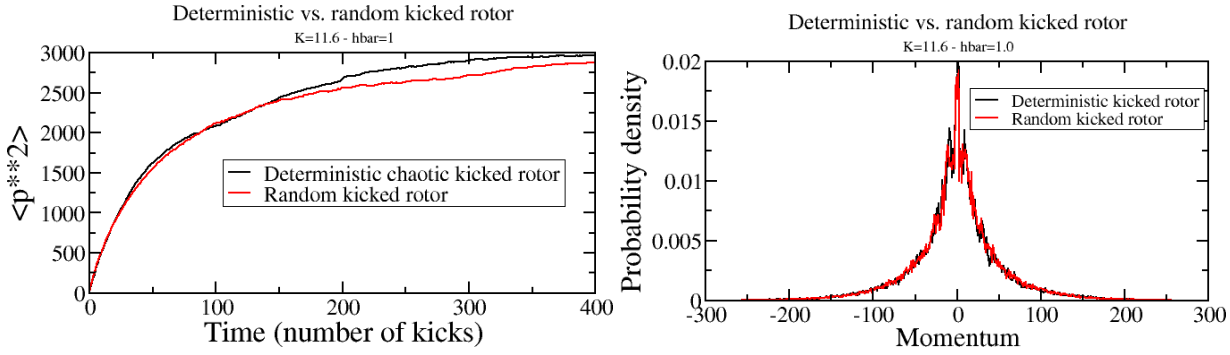

FIG. 8. Temporal evolution of $\langle p^2 \rangle$ (left) and average probability density in momentum space $|\psi(p)|^2$ (right) for the deterministic quantum kicked rotor and the random kicked rotor. They behave similarly, proving that it is the free propagation of the rotor between kicks which is the source of (pseudo-)randomness and disorder. Parameters are $K = 11.6, \hbar = 1.0$

where

$$\epsilon_m = \tan\left[\left(E - \tfrac{1}{2}m^2\hbar^2\right) T/2\hbar\right]. \tag{20}$$

Equation (19) is the time-independent Schrödinger equation for a one-dimensional Anderson model with site index m, on-site energy ϵ_m, coupling W_r to the nearest sites and total energy $-W_0$. There are two new ingredients compared to a standard Anderson model: firstly, there are additional hopping amplitudes to other neighbors. But since they decrease sufficiently fast at large distance, they do not play a major role. Secondly, the ϵ_m values, determined deterministically by (20), are not really random variables, but only pseudo-random[19] with a Lorentzian distribution.[20] Still, localization is expected and indeed observed.

This mapping shows that the on-site pseudo-randomness comes from the free propagation part of the evolution operator, while the non-random hopping between the sites originates from the kick operator. The statistical distribution of the ϵ_m in eq. (19) is a Cauchy (or Lorentz) distribution independently of k, while the hopping amplitudes increase with k. Thus, the weak disorder limit (hopping dominates randomness) of this on-site Anderson model is counterintuitively the large k limit where the classical dynamics is the most chaotic. Similarly, the strong disorder limit corresponds to small k (small hopping), so that the particles are essentially localized on a single site with a vaninshingly small localization length.

A consequence of this surprizing result is that the localization properties should not depend on the details of the free propagation part of the evolution operator. In other words, one could replace the determninistic diagonal phase factor $\exp(-im^2\hbar/2)$ by random uncorrelated phase factor $\exp(-i\phi_m)$ without affecting the localization properties. This modified system is called the random kicked rotor and numerical experiments show that is has similar localization properties, see figure 8.

The localization length $p_{\rm loc}$ can be approximately computed using the equivalence with an Anderson-like model (which is rather a Loyd model). We will use a different way to compute it, which gives (of course!) the same result.

There is a significant difference between time-independent and time-periodic systems. The former have a discrete pure point spectrum if the classical dynamics is bound; the latter usually have at least a dense spectrum. Indeed, the quasi-energy spectrum is defined modulo $2\pi\hbar/T$. Hence, there is an infinite number of energy levels in a finite energy range and the mean level spacing is not well defined. In fact, the quantity of interest is rather the local density of states, that is the density of states weighted by the overlap with the initial state, something like $\sum_i |c_i|^2\ \delta(E - E_i)$. Most of the Floquet eigenstates are so weakly overlapping with the initial state that it may happen that the effective density of states contributing to the dynamics is finite. In such a case, the Heisenberg time is just $2\pi\hbar$ times this effective density of states. But this is also the localization time $t_{\rm loc}$. Indeed, when it reaches $T_{\rm H}$, the system resolves the underlying Floquet spectrum and "knows" that it is discrete. It cannot thus explore new regions of phase space and the quantum dynamics freeze.

This is what happens for the kicked rotor. We can derive a rough estimate of the Heisenberg time. Suppose that the initial state is effectively coupled to ℓ Floquet states. Then, the mean level spacing is $2\pi\hbar/\ell$ and the Heisenberg time is:

$$T_{\rm H} = \ell. \tag{21}$$

After $T_{\rm H}$, the system has undergone a chaotic diffusion and thus reached a typical value (assuming $p \simeq 0$ initially):

$$\langle p^2 \rangle \simeq 2DT_{\rm H} = \frac{K^2}{2}\ \ell \tag{22}$$

Only states with sufficiently low m – such that $m^2\hbar^2 \leq \langle p^2 \rangle$ – will significantly contribute to the dynamics. The number of such states is, by definition, ℓ. This implies that:

$$2\ell^2\hbar^2 \simeq \frac{K^2}{2}\ \ell. \tag{23}$$

This determines:

$$\ell \simeq \frac{K^2}{4\hbar^2} \tag{24}$$

and the localization length in momentum space:

$$p_{\rm loc} = \ell\hbar \simeq \frac{D}{\hbar} = \frac{K^2}{4\hbar} \tag{25}$$

The localization time is in turn given by:

$$t_{\rm loc} = T_{\rm H} \simeq \frac{D}{\hbar^2} = \frac{K^2}{4\hbar^2} \tag{26}$$

These estimates agree well with the numerical observations. For truly quantitative results, the full approximate expression for the diffusion constant D, eq. (10) should be used.

In the semiclassical limit, both the localization length (actually in the momentum space) and the localization time diverge, which means that dynamical localization disappears.

Note: the script `pseudo_random_sequence.py` computes the pseudo-random sequence ϵ_m. The script `kr_periodic.py` can also compute the temporal evolution of the random kicked rotor (set the variable `random_kicked_rotor` to `True`).

II. LECTURE II: EXPERIMENTS WITH THE PERIODICALLY KICKED ROTOR

A. Keys for a successful experiment

From the first lecture, we know what is really important and what it less important for a possible experimental observation of dynamical localization. The essential ingredients are:

- One-body Hamiltonian without internal degrees of freedom;
- 1d dynamics;
- Time-periodic Hamiltonian;
- Spatially periodic Hamiltonian (periodic potential);
- Phase coherence over long time;
- Sufficiently large number of kicks;
- Incommensurability of the effective dimensionless $\hbar$ with 2π.

Less important points are:

- Kicks (mainly for convenience of the calculation);
- Dispersion relation;
- Well defined initial state, as long as it is smaller than the localization length.

The spatial periodicity implies to use some kind of lattice, an optical lattice when we use cold atoms.

The external dynamics of cold atoms in an optical lattice can satisfy all these constraints: the atomic internal degrees of freedom can be forgotten, and the versatility of atom-laser interaction makes it possible to build a fully externally controlled effective Hamiltonian. The time and length scales are favorable: the typical quantum time scale for cold atoms is the inverse of the recoil energy, that is around 100 microseconds. The typical length scale is the wavelength of the laser light used to manipulate the cold atoms, that is a fraction of a micro-meter. The associated velocity if of the order of 1 cm/s. All these orders of magnitude are rather easily reached with standard experimental techniques.

B. Atom-light interaction - Optical potential

Consider a two level atom interacting with a laser of frequency $\omega_L = k_L c$ detuned by $\Delta_L = \omega_L - \omega_0$ from the atomic transition of frequency ω_0. It is well known that there are two kinds of interactions between the atom and the radiation: Firstly, the atom can absorb a photon from the laser and re-emit it spontaneously in a random direction. This is a dissipative process giving rise to radiation pressure force, whose rate is $\Gamma\Omega^2/4\Delta_L^2$ where Γ is the natural width and Ω the resonant Rabi frequency (we assume $|\Delta_L| \gg \Gamma$). Secondly, the atom can pick a photon in a laser mode and emit it by stimulated emission. This conservative process is associated with a potential acting on the atom's center of mass motion, called the optical or dipole potential, whose value is:

$$V_{\text{opt}} = \frac{\hbar\Omega(\mathbf{r})^2}{4\Delta_L} \tag{27}$$

where $\mathbf{r}$ is the atom center of mass position. Being proportional to the square of the Rabi frequency, it is directly proportional to the laser intensity at position $\mathbf{r}$.

How to create a spatially modulated potential (for the kicks) thus requires a spatially modulated intensity, which is easily done with a standing wave. Clearly, this interaction is one dimensional, as momentum exchanges between the atom and the radiation are always along the standing wave: The atom absorbs a photon in one of the propagating beams and emits it in the counterpropagating beam, leading to a quantized momentum exchange of $2\hbar k_L$ along the laser axis. An important point is that the optical potential amplitude scales as Ω^2/Δ_L whereas the spontaneous emission rate scales as $\Gamma\Omega^2/\Delta_L^2$. In the regime $|\Delta_L| \gg \Gamma$, the optical potential is the dominant contribution to the dynamics, with spontaneous emission events being rare. Moreover, one can reduce the spontaneous emission rate by increasing the detuning Δ_L, provided that the laser has enough power to keep the potential amplitude at the required level.

C. The atomic kicked rotor

Suppose now that, instead of having the atom interacting continuously with the standing wave, one modulates the radiation intensity periodically (with period T_1) so that it is on for a short time τ (as compared to the atom dynamics) and off the rest of the period. One then obtains the Hamiltonian:

$$H = \frac{P^2}{2M} + \frac{\hbar\Omega^2\tau}{8\Delta_L}\cos(2k_L X)\sum_n \delta_\tau(t' - nT_1) \tag{28}$$

where $\delta_\tau(t) = 1/\tau$ if $|t| \leq \tau/2$ and zero otherwise. This functions tends to the Dirac δ-function as $\tau \to 0$.

It is useful to introduce a set of scaled, dimensionless units [14]:

$$\begin{aligned} x &= 2k_L X \\ p &= 2k_L T_1 P/M \\ t &= t'/T_1 \\ K &= \frac{\hbar\Omega^2 T_1 \tau k_L^2}{2M\Delta_L} \\ \hbar_{\text{eff}} &= 4\hbar k_L^2 T_1/M \\ \mathcal{H} &= \frac{4k_L^2 T_1^2}{M} H \end{aligned} \tag{29}$$

In the limit of short pulses $\tau \ll T_1$, one then has:

$$\mathcal{H} = \frac{p^2}{2} + K\cos x \sum_n \delta(t - n) \tag{30}$$

which is precisely the Hamiltonian of the kicked rotor. One has thus realized an atomic kicked rotor [15]. The above Hamiltonian is associated with the Schrödinger equation:

$$i\hbar_{\text{eff}}\frac{\partial\psi}{\partial t} = \mathcal{H}\psi. \tag{31}$$

$\hbar_{\rm eff}$ (sometimes noted $\bar{k}$) plays the crucial role of an effective Planck constant, which can be adjusted at will by modifying e.g. the period T_1. The interesting physics takes place in the momentum space. The scaling Eqs. (29) is such that $P = 2\hbar k_L$ corresponds to $p = \hbar_{\rm eff}$. If the atom is cold enough that its typical momentum is comparable to $2\hbar k_L$ (the "quantum" of momentum exchange), quantum effects can be observed in the system. Fortunately, magneto-optical traps produce atoms with a typical momentum of a few $\hbar k_L$. It is customary to measure the atomic momentum P in units of $2\hbar k_L$, i.e. measure p in units of $\hbar_{\rm eff}$.

The spatial dimensions perpendicular to the laser beams do not play any role in the problem, so that we have an effectively one-dimensional time-dependent problem. The mapping of the dimensionfull Hamiltonian for cold atoms to the kicked rotor Hamiltonian shows that the effective Planck's constant of the problem is $\hbar_{\rm eff} = 8\omega_r T$, that is 8 times the ratio of the atomic recoil frequency ω_r to the pulse frequency, and can be easily varied in the experiment, from the semiclassical regime $\hbar_{\rm eff} \ll 1$ to the quantum regime $\hbar_{\rm eff} \sim 1$.

There is however a slight complication: the configuration space of the atomic kicked rotor is the full x axis, not the $[0, 2\pi]$ interval of the model system. Thus, the wavefunction in configuration space is not 2π-periodic. The Bloch theorem gives the solution of this problem. Instead of using strictly 2π-periodic functions, one can expand any (non periodic) wavefunction in the basis of Bloch waves, which are products of 2π-periodic functions by a plane wave $\exp(i\beta x)$ characterized by the quasi-momentum $\hbar\beta$, β taking any value in the interval $[-0.5, 0.5[$ (first Brillouin zone). Because the spatial potential is periodic, the temporal evolutions of the various β components are independent. The only price to pay is the replacement of the integer m characterizing the momentum eigenstates by $m + \beta$ in the various equations above. In particular, different β produce different realizations of the on-site disorder of the equivalent Anderson model:

$$\epsilon_m = \tan\left[\left(E - \tfrac{1}{2}(m+\beta)^2\hbar^2\right) T/2\hbar\right]. \tag{32}$$

In other words, the distribution of quasi-momentum performs the disorder averaging for free! This is why the experimental signals do not display the same large fluctuations than the numerical calculations for the pure kicked rotor keeping $\beta = 0$.

D. Experimental observation of dynamical localization

The simplest observation uses a cold atomic gas, prepared in a standard magneto-optical trap with a typical velocity spread of few recoil velocities [6, 7, 16]. After the trap is switched off, a periodic train of laser pulses is applied to the atoms. Each pulse is composed of two far-detuned counter-propagating laser beams producing a spatially modulated optical potential. Each laser pulse thus produces a kick on the atom velocity, whose amplitude is proportional to the gradient of the optical potential.

After the series of pulses is applied, the momentum distribution is measured either by a time of flight technique [6] or velocity selective Raman transitions [7]. Fig. 9 shows the average value $\langle p^2\rangle$ as a function of time (number of kicks). One clearly sees a linear growth at short time followed by a saturation, that is a freezing of the diffusive growth when dynamical localization takes place.

Figure 10 shows the momentum distribution as a function of time. While, at short time, the distribution is Gaussian—as expected for a classical diffusion—, its shape changes around the localization time and evolves toward an exponential shape $\exp(-|p|/p_{\rm loc})$ at long time, a clear-cut manifestation of Anderson/dynamical localization.

The parameters used in this experiment (Na atoms, $K = 11.6$, $\hbar = 2.0$) are such that the theoretical prediction is a localization time of 8.3 kicks, in good agreement with numerical experiments and the experimental observation. The saturation level of $\langle p^2\rangle$ at long time is also quantitatively predicted.

E. Experimental imperfections - Decoherence effects

The experiments of course suffer from several imperfections and limitations. It is the simultaneous minimization of all these drawbacks that dictate the optimal experimental parameters.

A first limitation is the finite duration of the kicks, which puts an upper limit on the atomic velocities. Indeed, if the atom is sufficiently fast to travel a significant fraction of the spatial period when the laser standing wave is switched on, the kick approximation breaks down. This leads to a reduction of the diffusion constant for fast atoms which could mimick Anderson localization. This is why more recent experiments use heavier (hence slower) atoms like Cs.

More importantly, there are several microscopic phenomena that can kill the phase coherence of the atomic wavefunction. The most important ones are:

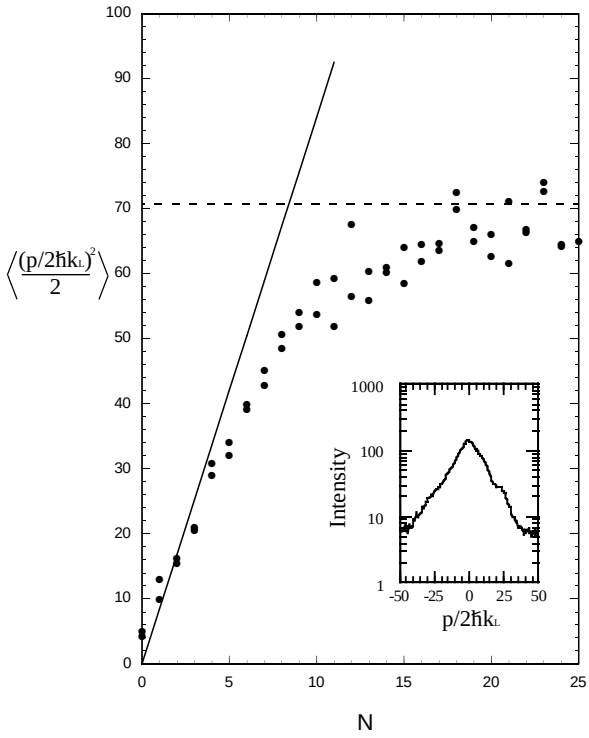

FIG. 9. Average value $\langle p^2 \rangle$ for a collection of cold atoms exposed to a series of kicks, as a function of time (the number of kicks). The solid line shows the linear growth predicted by theory at short time (classical chaotic diffusion). The dashed line is the saturation value predicted by dynamical localization and the dots are the experimental observation. The inset shows the final momentum distribution on a logarithmic scale, see also Fig. 10 (courtesy of M. Raizen).

- Collision between atoms. An elastic collision produces a local (in space) phase shift that breaks the global phase coherence in momentum space. This is why a rather dilute atomic gas must be used. The rate is typically around 1 collision every few hundred kicks.

- Spontaneous emission. When an atom spontaneously scatters a photon in a mode which is not one of the laser modes, it picks a random recoil (depending on the direction of emission). This leads to an additional phase factor $\exp(ip_{recoil}x)$ in the atomic wavefunction, i.e. a random shift of the quasi-momentum. After such an event, the precise phase relations between momentum components which ensure localization are no longer satisfied and classical diffusion restarts, as shown in figure 11. By increasing the detuning of the laser (and increasing simultaneously its intensity), one can limit this process to few thousandths per kick.

- Noise on the kick strength. The kick strength may fluctuate from one kick to the next kick. Although this is not strictly decoherence, but rather a Hamiltonian random dephasing process, it also can kill dynamical/Anderson localization.

- Because of gravity, the atoms fall and tend to escape the horizontal laser beam, again breaking temporal periodicity. This limits the duration of the kicking sequence to about 200 kicks.

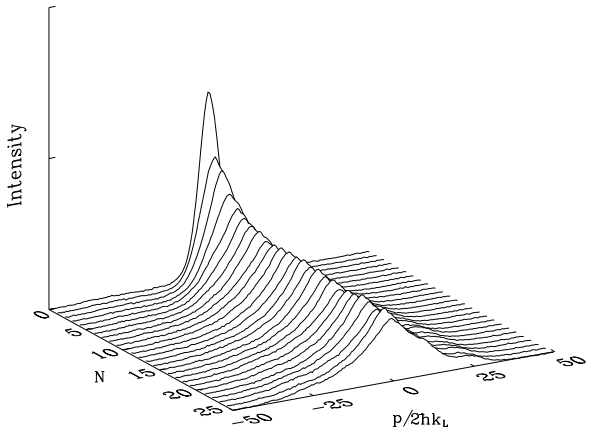

FIG. 10. Experimental time evolution of the momentum distribution of the atomic kicked rotor [6], from the initial Gaussian distribution until the exponentially localized distribution at long time; N is the number of kicks (courtesy of M. Raizen).

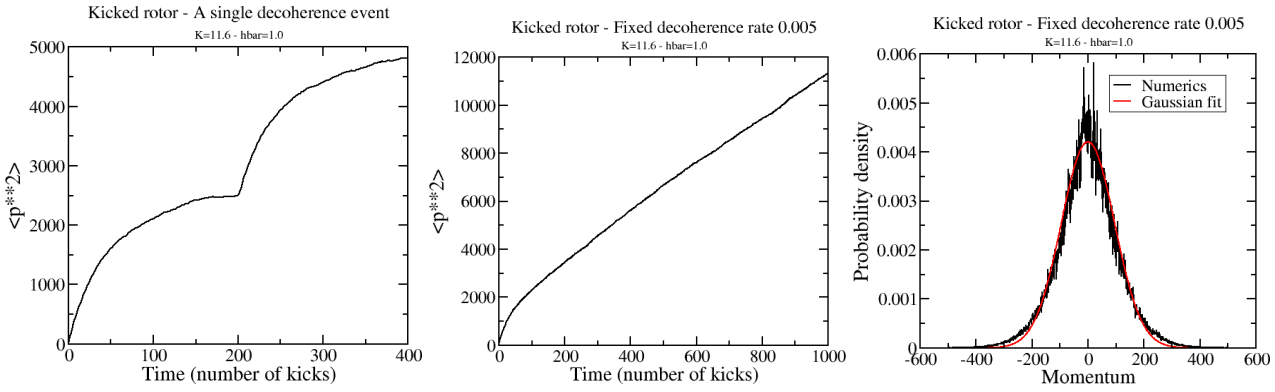

FIG. 11. Modelization of the effect of a decoherence process, such as spontaneous emission, on dynamical/Anderson localization. A single decoherence event (left) destroys phase coherence and classical diffusion restarts until localization sets is again on a longer scale. When decoherence events occur randomly in time, this recreates a global diffusion (middle) with a diffusion constant smaller than the classical diffusion constant, and the momentum distribution tends to a Gaussian (right).

- If the laser beam is not perfectly horizontal, there is a residual linear potential along the laser axis which breaks spatial periodicity, and hence dynamical/Anderson localization.

All these effects limited the coherence time to few tens of kicks in the first generation of experiments. As will be discussed in Lecture III, this is too short to allow for observing Anderson localization in dimension higher than 1. Fortunately, improvements in the experimental setups has now pushed this limit to several hundred kicks, and the next generation could reach 1000 kicks or more, opening the way to new experiments.

Decoherence can be modelled by events which brutally kills the phase coherence (or by small dephasing effects leading to progressive loss of phase coherence). The effect on dynamical/Anderson localization is shown in figure 11. It is important to note that a decoherence rate larger than the inverse of the localization time will make the unambiguous observation of localization quite difficult. When the decoherence rate γ is small compared to the localization time $t_{\rm loc}$, the residual diffusion constant is simply [16]:

$$D^* = D_{\rm classical}\ \gamma\ t_{\rm loc}. \tag{33}$$

A controlled addition of decoherence has been performed in real experiments. Adding decoherence on the system—either by adding spontaneous emission [16] or by weakly breaking the temporal periodicity [17]—induces some residual diffusion at long time, see figures 12 and 13. This is another proof that dynamical localization is based on delicate destructive interference.

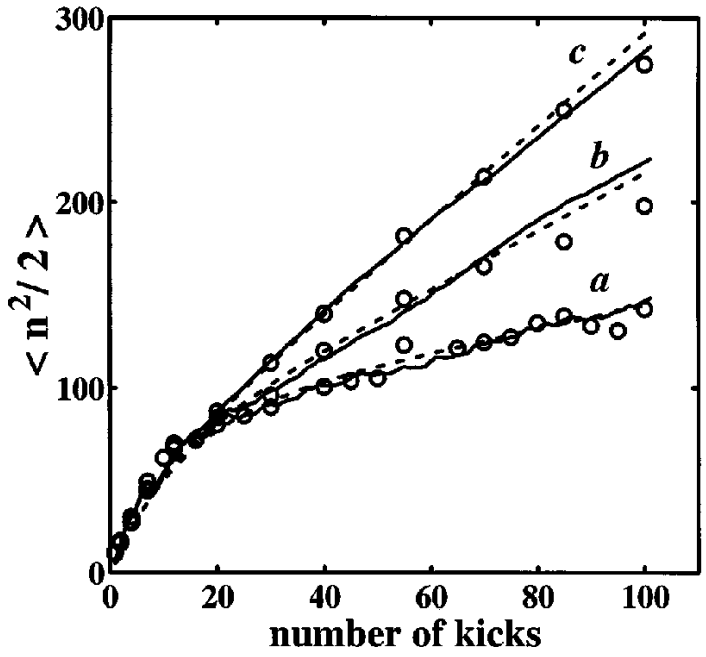

FIG. 12. Average value $\langle p^2 \rangle$ as a function of time (the number of kicks), in the presence of decoherence, due to spontaneous emission of photons by the atoms. At long time, decoherence restore a diffusive behaviour, albeit with a diffusion constant smaller than predicted by classical mechanics. The various curves correspond to various decoherence rates (courtesy of H. Ammann).

Note: the scripts `kr_periodic_with_one_decoherence_event.py`, `kr_periodic_with_fixed_decoherence_rate.py` and `kr_periodic_with_noise.py` are various models for decoherence and noise, showing the appearance of a global residual diffusion at long time.

III. LECTURE III: THE QUASI-PERIODICALLY KICKED ROTOR

[1] J. Billy, V. Josse, Z. Zuo, A. Bernard, B. Hambrecht, P. Lugan, D. Clément, L. Sanchez-Palencia, Ph. Bouyer and A. Aspect, "Direct observation of Anderson localization of matter waves in a controlled disorder", Nature **453**, 891-894 (12 June 2008); Ph. Bouyer *et al.*, "Anderson localization of matter waves", Proceedings of the XXI ICAP Conference, R. Coté, Ph. L. Gould, M. Rozman and W. W. Smith eds., World Scientific (2008).

[2] P. W. Anderson, "Absence of Diffusion in Certain Random Lattices", Phys. Rev. **109**, 1492 (1958)

[3] E. Abrahams, P. W. Anderson, D. C. Licciardello and T. V. Ramakrishnan, "Scaling Theory of Localization: Absence of Quantum Diffusion in Two Dimensions", Phys. Rev. Lett. **42**, 673 (1979)

[4] S.S. Kondov et al, Science **334**, 66 (2011).

[5] F. Jendrzejewski et al., Nature **8**, 398 (2011).

[6] F.L. Moore, J.C. Robinson, C. Bharucha, P.E. Williams and M.G. Raizen, "Observation of Dynamical Localization in Atomic Momentum Transfer: A New Testing Ground for Quantum Chaos", Phys. Rev. Lett. **73**, 2974 (1994)

[7] J. Chabé, G. Lemarié, B. Grémaud, D. Delande, P. Szriftgiser and J.C. Garreau, "Experimental observation of the Anderson metal-insulator transition with atomic matter waves" Phys. Rev. Lett. **101**, 255702 (2008).

[8] M. Lopez, J.F. Clément, P. Szriftgiser, J.C. Garreau and D. Delande, Phys. Rev. Lett. **108**, 095701 (2012), arXiv:1108.0630: "Experimental Test of Universality of the Anderson Transition"

[9] G. Lemarié, H. Lignier, D. Delande, P. Szriftgiser and J.C. Garreau, Phys. Rev. Lett. **105**, 090601 (2010), arXiv:1005.1540: "Critical State of the Anderson Transition: Between a Metal and an Insulator"

[10] A.J. Lichtenberg and M.A. Lieberman, *Regular and stochastic motion*, Springer-Verlag, New-York (1983).

[11] G. Casati, I. Guarneri and D. Shepelyansky, Physica A **163**, 205 (1990) and references therein.

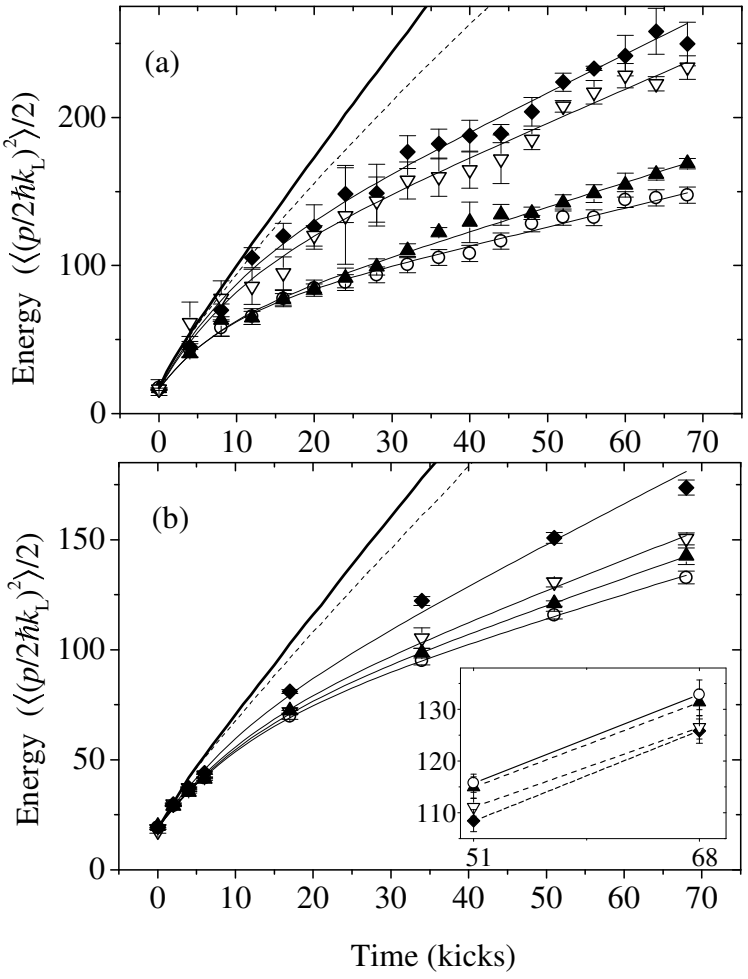

FIG. 13. Average value $\langle p^2 \rangle$ as a function of time (the number of kicks), in the presence of amplitude noise for the kicks (a) or spontaneous scattering of photons (b). Both effects destroy dynamical localization and partly restore the classical diffusive behaviour. The various curves correspond to various levels of noise or inelastic process. In each figure, the upper thick line is the classical behaviour (courtesy of M. Raizen).

[12] G. Casati, B.V. Chirikov, J. Ford and F.M. Izrailev, "Stochastic Behavior of Classical and Quantum Hamiltonian Systems", Lecture Notes in Physics, **334**, G. Casati and J. Ford eds., Springer, New York (1979).

[13] D.R. Grempel, R.E. Prange and S. Fishman, Phys. Rev. A **29**, 1639 (1984).

[14] G. Lemarié, J. Chabé, P. Szriftgiser, J.C. Garreau, B. Grémaud and D. Delande, "Observation of the Anderson Metal-Insulator Transition with Atomic Matter Waves: Theory and Experiment", Phys. Rev. A **80**, 043626 (2009).

[15] F. L. Moore, J. C. Robinson, C. F. Bharucha, B. Sundaram, and M. G. Raizen, "Atom Optics Realization of the Quantum δ-Kicked Rotor", Phys. Rev. Lett. **75**, 4598 (1995).

[16] H. Ammann, R. Gray, I. Shvarchuck and N. Christensen, Phys. Rev. Lett. **80**, 4111 (1998).

[17] B.G. Klappauf, W.H. Oskay, D.A. Steck and M.G. Raizen, Phys. Rev. Lett. **81**, 1203 (1998).

[18] In the literature, the localization length is defined as the characteristic length for the decay of either $|\psi|^2$ or of $|\psi|$. The two quantities of course differ by a factor 2. Usage of one or the other definition depends on the community, but may also fluctuate from paper to paper. One has to live with this source of disorder.

[19] As is well known, "random-number generators" implemented in computers also generate deterministic, merely pseudo-random sequences; most of them use formulae analogous to (20).

[20] The non-random character appears for example, when the product $\hbar T/2$ is chosen as an integer multiple of 2π. Then all ϵ_m are equal, the motion is ballistic and localization is absent. Similarly, when $\hbar T$ is commensurate with π (the so-called quantum resonances), the sequence ϵ_m becomes periodic, and Anderson localization does not take place, giving way to Bloch-band transport.